

Improvements of Side Oblique Pole Impact Safety Performance using Finite Element Method

Selvamanikandan M

PG Scholar, Department of Mechanical Engineering
VMKV Engineering College
Salem, India

Venkatesan S

Professor, Department of Mechanical Engineering
VMKV Engineering College
Salem, India

Abstract— Side Pole impacts are the most severe injury crash in the automotive passenger vehicle. This critical happened due to very narrow impact location (pole) and very less crush space available in the side structure of the vehicle. There are many ways to measure the side pole crash performance of the vehicle. That is 90 degree impact and inclined impact. In this study, 75deg inclined pole impact has considered. The vehicle with its curb mass moving laterally at a speed of 32kmph and impacts with a pole at H Point of driver location in the vehicle with 75deg inclination. From this study, clearly understand the important load path members and Enablers introduced to improve the side pole crash performance. In this paper, according to UN-R135, side oblique pole impact was conducted and with improvement enabler's result has compared.

Keywords—Side Pole impact; Oblique Impact; Occupant safety; Automotive crash; UN-R135; FMVSS 214; SUV Pole Impact.

I. INTRODUCTION

The best way to develop the automotive safety is avoiding the crash with active safety systems such as like brake, warning devices, cameras and sensors. But every year the no of vehicle on the road is increasing, this increasing the road accidents also. Asper WHO report averagely 2900 deaths per day occurring due to road accidents. Crashworthiness is the ability to absorb the crash energy with in the structure and transfer as minimum as energies to the occupant and reducing the injury.

Most of the time when vehicle experiencing side crashes, there is less stiffness to resist the structure deformation. This is due to the side structure has very minimal crush space to absorb the energy, So by introducing side door beams was transferring the impact energy to other BIW parts and reducing the door deformation. For this side door beam also investigated by the way of various sectional analysis and best optimal member selected to improve the side impact performance [4].

Currently all the countries trying to develop better Electric Vehicle. But electric vehicle should meet in the Occupant protection and structural safety performance with electrical safety performance. The battery pack installed on the bottom middle position of the vehicle. Side pole impact is the worst case for this battery pack. And this impact conducted by reviewing the results, Battery box body structure strengthened of special processing, to avoid cells to be squeezed and shifted [5].

In every country has high rank in side impact accidents. Automotive industries are more focused on the vehicle side

structure energy absorption. In the pole impact objective is to maintain the integrity of the occupant compartment area and avoid the impacts on the head [6].

II. FINITE ELEMENT MODEL DETAILS

FE Model of Vehicle was disassembled and verified with BOM thickness and material information. Full view of vehicle shown in the Fig 1 and 2. Full vehicle model has converted from design model to the FEA model by using appropriate elements and joints.

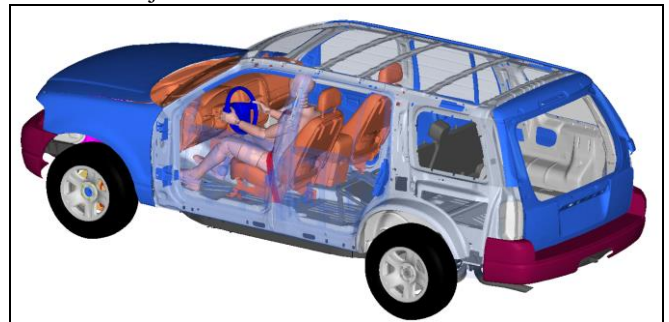


Fig. 1. Vehicle FE Model ISO View

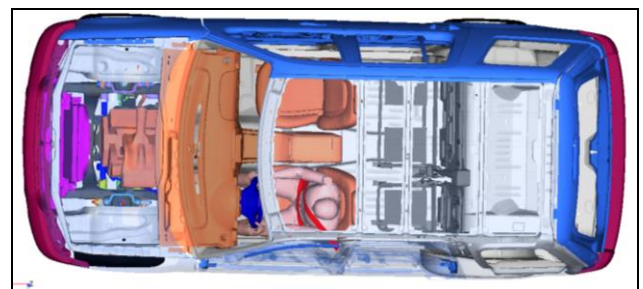


Fig. 2. Vehicle FE Model Top View

A. Elements types and Quality

The sheet parts of the vehicle has model with shell elements (Quad and Triangular). The meshing has made in the mid plane of the components and thickness assigned to that elements, these elements will extrude both side equally to represent the thickness. Casting parts, thickness more than 6mm parts, foam has modelled with hexa penta elements. Bolts are model with 1D-beam elements with corresponding diameters. Welds are represented by using DYNA SPOT Weld elements. All joints of vehicle modelled with appropriate joints like Spherical joint, revolute joint, universal joint, Translation Joint, and lock Joints. All element Types with their counts has shown in the Fig 4. Elements average

size is 5mm. and the quality parameters are shown in the Fig 3.

▼ ELEMENT	904726
ELEMENT_BEAM_ELFORM_1	185
ELEMENT_BEAM_ELFORM_2	258
ELEMENT_BEAM_ELFORM_3	52
ELEMENT_BEAM_ELFORM_6	45
ELEMENT_DISCRETE	46
ELEMENT_MASS	478
ELEMENT_SEATBELT	283
ELEMENT_SEATBELT_ACCELEROMETER	14
ELEMENT_SEATBELT_SLIPRING	1
> ELEMENT_SHELL	752808
> ELEMENT_SOLID	149958
ELEMENT_TSHLL	598

Fig. 3. FE Elements Types and counts













Target element size:		5,000	
Calculation method:		OptiStruct	
<input checked="" type="checkbox"/> <input type="checkbox"/> <input type="checkbox"/> <input type="checkbox"/> <input type="checkbox"/> <input type="checkbox"/> <input checked="" type="checkbox"/> Advanced			
<input checked="" type="checkbox"/>	On	Color	Fail
1	<input checked="" type="checkbox"/> Minimum size		Minimal normalized height 2,000
2	<input checked="" type="checkbox"/> Maximum size		20,000
3	<input checked="" type="checkbox"/> Aspect ratio		OptiStruct 5,000
4	<input checked="" type="checkbox"/> Warpage		OptiStruct 15,000
5	<input checked="" type="checkbox"/> Maximum interior angle quad		140,000
6	<input checked="" type="checkbox"/> Minimum interior angle quad		40,000
7	<input checked="" type="checkbox"/> Maximum interior angle tria		120,000
8	<input checked="" type="checkbox"/> Minimum interior angle tria		30,000
9	<input checked="" type="checkbox"/> Skew		OptiStruct 40,000
10	<input checked="" type="checkbox"/> Jacobian		At integration points 0,600
11	<input type="checkbox"/> Chordal deviation		1,000
12	<input checked="" type="checkbox"/> Taper		OptiStruct 0,600
13	<input checked="" type="checkbox"/> % of trias		15,000

Fig. 4. 2D Element Quality parameters

B. Constrained Connections

In the vehicle connection, Joints, extra nodes, Nodal Rigid Bodies and spot weld options has used. Joints used to represent the actual joints in the physical vehicle. Additional Extra Node option for connecting rigid parts with deformable parts. With NRB, the bold connection and another connection location were modelled. Spot weld connection to represent the physical spot with the actual diameter. Complete vehicle spot welding highlighted in Fig 6.

▼ CONSTRAINED	9719
CONSTRAINED_JOINT_UNIVERSAL	2
CONSTRAINED_JOINT_CYLINDRICAL	3
CONSTRAINED_EXTRA_NODES_NODE	20
CONSTRAINED_JOINT_SPHERICAL	21
CONSTRAINED_JOINT_STIFFNESS_GENERALIZED	27
CONSTRAINED_JOINT_REVOLUTE	61
CONSTRAINED_RIGID_BODIES	112
CONSTRAINED_EXTRA_NODES_SET	187
CONSTRAINED_NODAL_RIGID_BODY	2444
CONSTRAINED_SPOTWELD	6842

Fig. 5. Constrained Connections

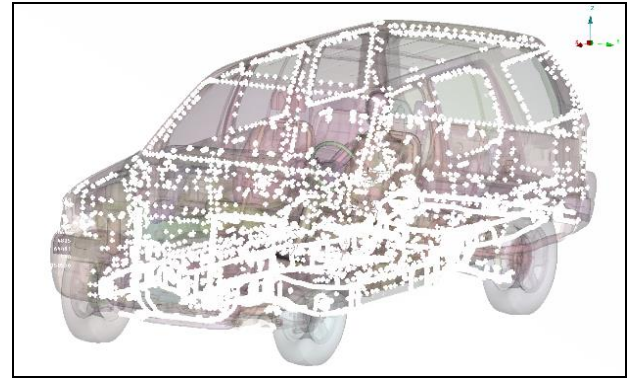


Fig. 6. Constrained Spot weld in BIW

C. LS-DYNA Non Linear Material Modeling

LS Dyna has comprehensive material library, in the vehicle components are made with lots of different material, which should model in the FEA with appropriate material card, also the rate of loading should be considered for high impact simulations. If some mistake modelling of material will lead to large changes in the behavior of components. All list of material card used in the model shown in the Fig 7. Elastro-plastic materials are modelled with MAT24 card, with strain rate dependent stress strain curves.

MATERIAL	1135
MAT71 MAT_CABLE_DISCRETE_BEAM	1
MAT_B01 MAT_SEATBELT	1
MAT_S02 MAT_DAMPER_VISCOUS	1
MAT26 MAT_HONEYCOMB	2
MAT123 MAT_MODIFIED_PIECEWISE_LINEAR_PLASTICITY	2
MAT_S05 MAT_DAMPER_NONLINEAR_VISCOUS	2
MAT83 MAT_FU_CHANG_FOAM	3
MAT_S01 MAT_SPRING_ELASTIC	4
MAT_S04 MAT_SPRING_NONLINEAR_ELASTIC	4
MAT3 MAT_PLASTIC_KINEMATIC	7
MAT6 MAT_VISCOELASTIC	14
MAT77 MAT_OGDEN_RUBBER	14
MAT66 MAT_LINEAR_ELASTIC_DISCRETE_BEAM	16
MAT7 MAT_BLATZ-KO_RUBBER	17
MAT57 MAT_LOW_DENSITY_FOAM	23
MAT1 MAT_ELASTIC	82
MAT9 MAT_NULL	90
MAT20 MAT_RIGID	301
MAT24 MAT_PIECEWISE_LINEAR_PLASTICITY	551

Fig. 7. Material Card details

2000112 MAT_PLASTIC111	210000	7.89E-9	2000113	370	MAT24 MAT_PIECEWISE_LINEAR_PLASTICITY
2000113 MAT_PLASTIC112	210000	7.89E-9	2000114	370	MAT24 MAT_PIECEWISE_LINEAR_PLASTICITY
2000114 MAT_PLASTIC113	210000	7.89E-9	2000115	370	MAT24 MAT_PIECEWISE_LINEAR_PLASTICITY
2000115 MAT_PLASTIC114	210000	7.89E-9	2000116	240	MAT24 MAT_PIECEWISE_LINEAR_PLASTICITY
2000116 MAT_PLASTIC115	210000	7.89E-9	2000117	240	MAT24 MAT_PIECEWISE_LINEAR_PLASTICITY
2000117 MAT_PLASTIC116	210000	7.89E-9	2000118	240	MAT24 MAT_PIECEWISE_LINEAR_PLASTICITY
2000118 MAT_PLASTIC117	210000	7.89E-9	2000119	240	MAT24 MAT_PIECEWISE_LINEAR_PLASTICITY
2000119 MAT_PLASTIC118	210000	7.89E-9	2000120	240	MAT24 MAT_PIECEWISE_LINEAR_PLASTICITY
2000120 MAT_PLASTIC119	210000	7.89E-9	2000121	240	MAT24 MAT_PIECEWISE_LINEAR_PLASTICITY
2000121 MAT_PLASTIC120	210000	7.89E-9	2000122	240	MAT24 MAT_PIECEWISE_LINEAR_PLASTICITY
2000122 MAT_PLASTIC121	210000	7.89E-9	2000123	240	MAT24 MAT_PIECEWISE_LINEAR_PLASTICITY
2000123 MAT_PLASTIC122	210000	7.89E-9	2000124	240	MAT24 MAT_PIECEWISE_LINEAR_PLASTICITY
2000124 MAT_PLASTIC123	210000	7.89E-9	2000125	240	MAT24 MAT_PIECEWISE_LINEAR_PLASTICITY
2000125 MAT_PLASTIC124	210000	7.89E-9	2000126	240	MAT24 MAT_PIECEWISE_LINEAR_PLASTICITY
2000126 MAT_PLASTIC125	210000	7.89E-9	2000127	370	MAT24 MAT_PIECEWISE_LINEAR_PLASTICITY
2000127 MAT_PLASTIC126	210000	7.89E-9	2000128	300	MAT24 MAT_PIECEWISE_LINEAR_PLASTICITY
2000128 MAT_PLASTIC127	210000	7.89E-9	2000129	200	MAT24 MAT_PIECEWISE_LINEAR_PLASTICITY
2000129 MAT_PLASTIC128	210000	7.89E-9	2000130	100	MAT24 MAT_PIECEWISE_LINEAR_PLASTICITY
2000130 MAT_PLASTIC129	210000	7.89E-9	2000131	200	MAT24 MAT_PIECEWISE_LINEAR_PLASTICITY
2000131 MAT_PLASTIC130	210000	7.89E-9	2000132	300	MAT24 MAT_PIECEWISE_LINEAR_PLASTICITY
2000132 MAT_PLASTIC131	210000	7.89E-9	2000133	370	MAT24 MAT_PIECEWISE_LINEAR_PLASTICITY
2000133 MAT_PLASTIC132	210000	7.89E-9	2000134	370	MAT24 MAT_PIECEWISE_LINEAR_PLASTICITY
2000134 MAT_PLASTIC133	210000	7.89E-9	2000135	370	MAT24 MAT_PIECEWISE_LINEAR_PLASTICITY
2000135 MAT_PLASTIC134	210000	7.89E-9	2000136	400	MAT24 MAT_PIECEWISE_LINEAR_PLASTICITY
2000136 MAT_PLASTIC135	210000	7.89E-9	2000137	400	MAT24 MAT_PIECEWISE_LINEAR_PLASTICITY
2000137 MAT_PLASTIC136	210000	7.89E-9	2000138	370	MAT24 MAT_PIECEWISE_LINEAR_PLASTICITY
2000138 MAT_PLASTIC137	210000	7.89E-9	2000139	370	MAT24 MAT_PIECEWISE_LINEAR_PLASTICITY
2000139 MAT_PLASTIC138	210000	7.89E-9	2000140	300	MAT24 MAT_PIECEWISE_LINEAR_PLASTICITY
2000140 MAT_PLASTIC139	210000	7.89E-9			

Fig. 8. MAT 24 Material Information

D. Assembly Mass and COG Information

The Mass of the vehicle has corrected with assembly level mass. Because kinetic energy of the vehicle depends on the vehicle mass also. The mass and center of gravity details are shown in the Table 1.

TABLE I. MASS AND COG DETAILS

S.No	Assembly	Mass (Kg)	COG
1	Chassis	317	X=-2543.16 Y=-8.4368 Z=415.307
2	All-Upper Body	954.2	X=-2522.26 Y=9.6351 Z=868.38
3	Engine & Transmission	363.3	X=-1090 Y=-7.6504 Z=630.188
4	Radiator	30.56	X=-360.53 Y=4.3557 Z=675.66
5	Fuel Tank	49.05	X=-2590.53 Y=279.75 Z=333.221
6	Front Power Train	50.22	X=-965.25 Y=88.53 Z=345.53
7	Rear Power Train	107.4	X= -3597.62 Y= 6.304 Z=378.72
8	Front-Wheel assembly	155.7	X= -828.955 Y= 3.57 Z=388.9117
9	Rear-Wheel assembly	184.5	X= -3700.92 Y=-1.4466 Z=364.149
10	Exhaust System	32.23	X=-2349.22 Y=222.468 Z=357.5
	TOTAL MASS	2244.16	

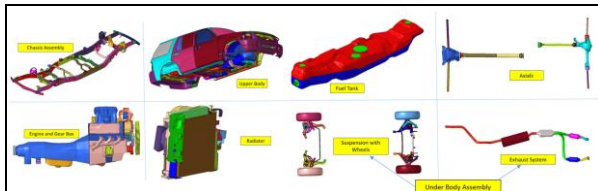


Fig. 9. Example of a figure caption. (figure caption)

III. SIDE OBLIQUE POLE IMPACT SETUP

Some side impacts happened a vehicle travelling sideways into rigid roadside barriers like trees or pole. Due to this result of loss of control and skid in slips condition. In the FMVSS 214, a car is propelled sideways at 32km/h against a rigid narrow pole. The car is positioned at an angle of 75degree from the vehicle longitudinal axis. A male WS 50% dummy positioned on the driver seat. This dummy has a mass of 78kg. This is very severe test of a car's ability to protect the driver's head injury. This pole placed at a position of driver H-Point location. The rigid pole has 254mm diameter.

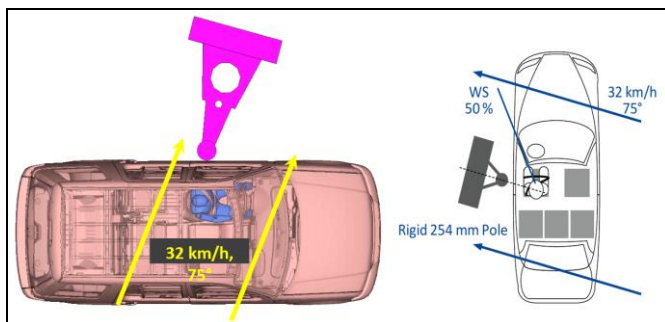


Fig. 10. Example of a figure caption. (figure caption)

IV. POLE IMPACT ENABLERS

In side pole impact collision cases, the load transfer from pole to the vehicle side structure, and then structure deforms and it contact with dummy pelvis location. Due to this structure to pelvis contact the load has transferred to the occupant. As only a very small crumple zone is available during a side pole impact, so we have to ensure that the impact forces are distributed over a wide area.

The B-Pillars and side members along the vehicles flanks are mainly responsible for this. Both components are partly manufactured from ultra-high strength, hot formed high steel. The impact forces are transferred from B Pillar to the opposite side of the vehicle first and foremost via the transversely rigid seat and the center console.

A further load dissipation path runs from the base of the B pillar to cross member under the seat and transmission tunnel braces.

Asper base line study, identified the important load transfer path members are B-Pillar and its reinforcements, Roof bows, Sill, Transfers cross members. These parts stiffness increased by the way of design changes and material grade up. The fig 11 shows the various stiffness increased parts.

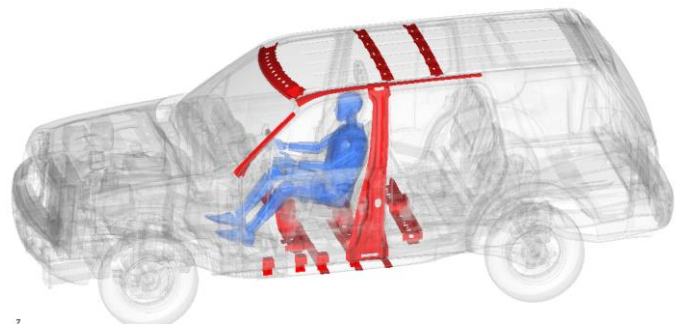


Fig. 11. Example of a figure caption. (figure caption)

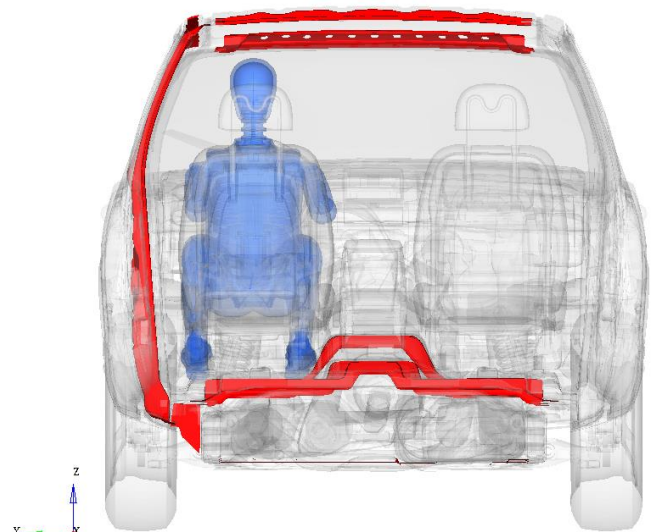


Fig. 12. Example of a figure caption. (figure caption)

V. ANALYSIS RESULTS

A. Deformation Mode

The overall deformation mode of the side oblique pole impact shown in the fig 13 and 14. In the right hand side picture is the base model and left side picture is improved vehicle. From the overall deformation mode the improved vehicle structural deformation significantly reduced. In the base vehicle A-pillar to B Pillar roof member experiencing large deformation, but in the improved vehicle it reduced considerably due to new reinforcement member.

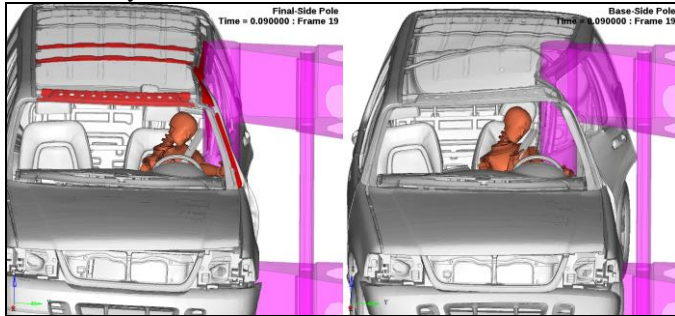


Fig. 13. Example of a figure caption. (figure caption)

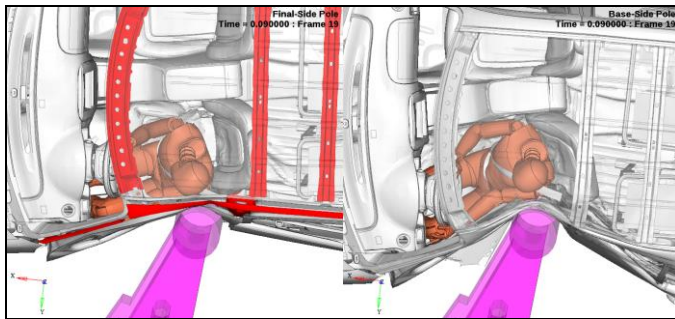


Fig. 14. Occupant Interaction during Side oblique Impact

B. BIW Deformation

The equations are an exception to the prescribed specifications of this template. BIW is the most important structure in the vehicle body, which connects the all other subsystems. The plastic strain of the BIW shown in the fig 15. From the strain contours, large deformation observed in the base vehicle B-Pillar and TWB locations. This deformation reduced on the improved model, due to the sill location and B-Pillar structural developments.

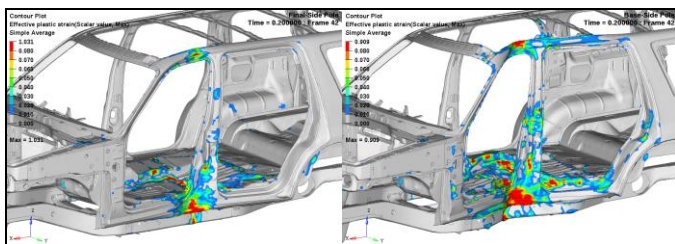


Fig. 15. BIW Plastic Strain deformation

In the BIW, Body side outer deformations measured with respect to the un-impact side. This measure curve profile shown in the fig 16. In the right side shown curve, Blue color

curve represent the base vehicle deformation profile and the red color curves represents the improved vehicle Intrusions. From the overlaid curve, improved vehicle intrusion significantly reduced compared with the base vehicle.

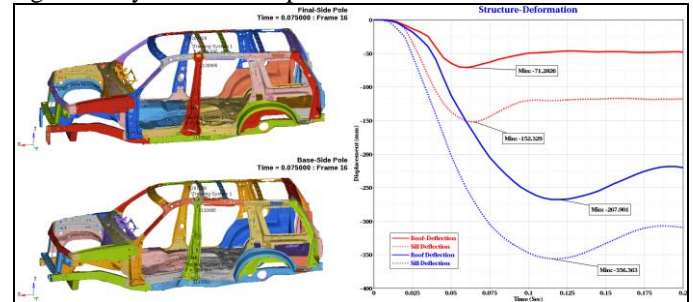


Fig. 16. Side Structure Intrusions

C. Underbody Deformation

The under body view of the vehicle shown in the fig 17. Right side picture for base vehicle and left side picture for improved vehicle. In the base vehicle large deformations observed in the frame at fuel tank cross member location. And frame bending lead to a catastrophic failure on the body structure, these failures improved by the side pole impact enablers as shown in the right side contour.

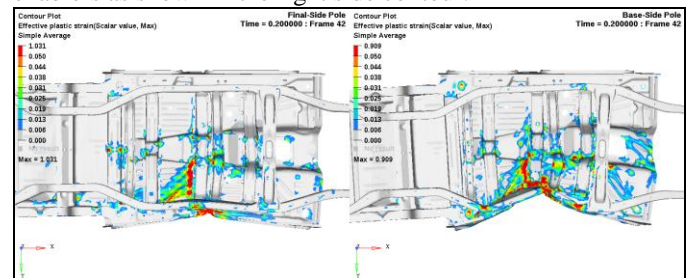


Fig. 17. Underbody Plastic strain Deformation

D. Seat Deformation

The first row seat structure shown in the fig 18. Seat structure is the one of major system for occupant safety, since occupant belted with the seat structure. In the strain contours showing the base vehicle seat structure experiencing large deformation. And this happened due to large load transferred from the side structure, this has eliminated due to side structure stiffness improved.

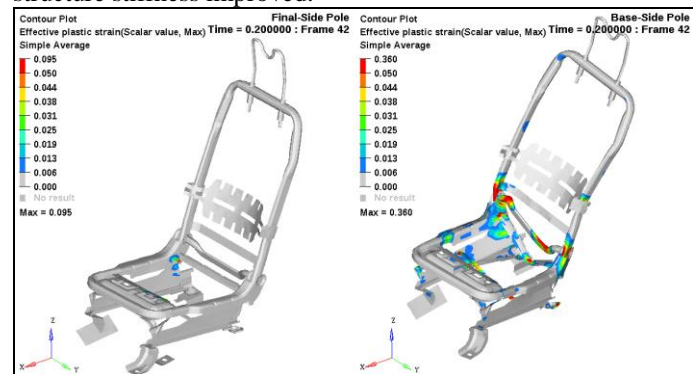


Fig. 18. Seat Structure Plastic deformation

Air bag gap closer measured during side pole impact. The seat back side cross member has a air bag to save the occupant from the lateral impact collision.

Also a curtain air bag placed on the side roof, to deploy these air bags, the side structure to seat must maintain certain gap. Otherwise the air bag will not deploy with effective manner. So always need to maintain certain gap between the side structures to the seat side members.

The fig 19 shows the comparison of gap closer measurement for Base vehicle with improved vehicle. Initial gap considered as 0mm, and the curve shows the side structure movement with respect to the seat side members. The final vehicle structure movement reduced significantly compared with base vehicle.

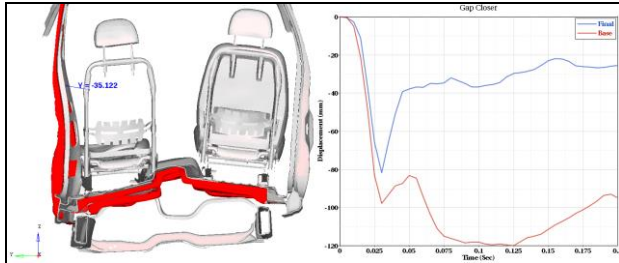


Fig. 19. Seat Air Bag Gap closer Measurement

E. B-Pillar Deformation

B-Pillar is the main load transfer member during side pole impact. This pillar section deformations measured with various points on the structure. The fig 20 shows the measured location on the BIW. The highlight black color points are measured coordinates for sectional deformation. This deformation shows the passenger compartment area integrity. Due to large deformation of B-Pillar section will transfer the more load in to the seat structure and occupants.

In the fig 21 shows the overlaid view of deformation, Black color curve represents the un deformed view of the structure, Blue color curve for Base vehicle deformation, red color curve represent the final improved vehicle deformation. From the fig 21, final vehicle deformation within the good target line, but it not maintained in the base vehicle.

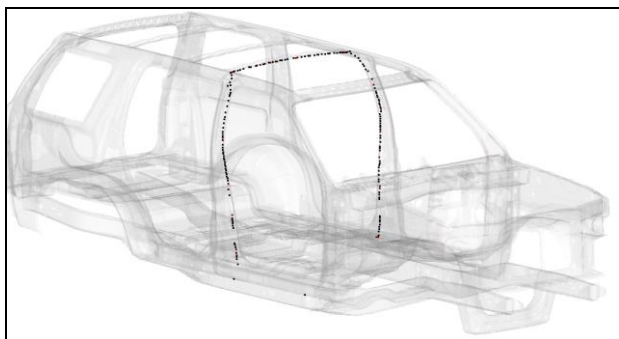


Fig. 20. Points for B-PLR Deformation section view

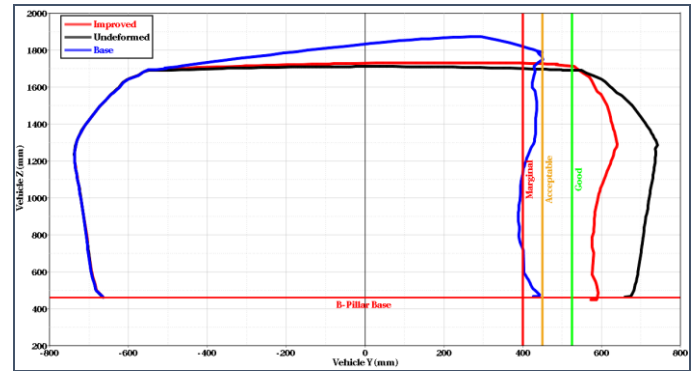


Fig. 21. B-PLR Deformation section view comparison

F. Roof Intrusion

The roof frame deformation modes are shown in the fig 22. This comparison view of roof deformation shown with undeformed wireframe mode. Roof frames are the important structure for curtain air bag. Because this air bag mounted with roof side frames, so this deformation will adjust the deployment gap, which lead to high deployment force or tearing on the air bag.

Large roof frames deformations are observed in the base vehicle. So the enablers introduced to reduce this roof frame deformation. After this structural improvements the deformation significantly reduced and improved the occupant safety level.

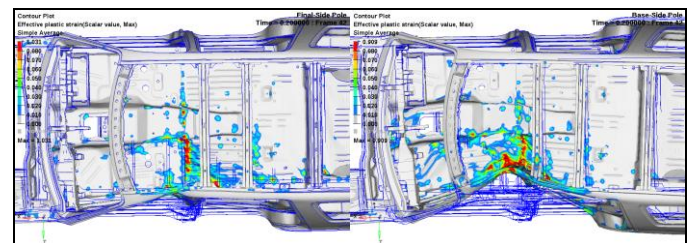


Fig. 22. Roof Deformation with Undeformed view

VI. CONCLUSION

The side oblique pole impact carried out for SUV vehicle. From the base model results identified the various load path members and sensitivity location. Also this results used to identify the suitable design countermeasures to reduce the occupant injuries and compartment intrusion. The high intrusions observed at the location of roof pillars and sill location on the base vehicle, to reduce this intrusion, roof pillar reinforcements and Sill L Members introduced on the final vehicle. These enablers added some additional mass to the vehicle.

ACKNOWLEDGMENT

The authors would like to thank Dr. S.Venkatesan, PG coordinator of VMKV Engineering College for encouraging these crash and safety research. In addition, the authors would like to acknowledge the contribution of CAE Industrial members for their strong support and guiding to do the safety research.

REFERENCES

- [1] Nithin S. Gokhale (2008), "Practical Finite Element Analysis" Finite to Infinite ISBN: 8190619500.
- [2] Federal Motor Vehicle Safety Standard FMVSS no.214.

-
- [3] Economic Commission for Europe Safety Regulation ECE r.135.
- [4] C.R.Long, S. Chung Kim Yuen, G.N. Nurick "Analysis of a car door subjected to side pole Impact" Latin American Journal of Solids and Structures, ISSN 1679-7825. 2019.
- [5] Zhu Haitao, Ji Yi, Zhing Yanhui "An Electric Vehicle (EV) Side Pole Collision Test Research" Applied Mechanics and Materials Vols.556-562 (2014) PP 1245-1250.
- [6] Wang Dazhi, Dong Guang, Zhang Jinhuan, Huang Shilin "Car Side Structure Crashworthiness in Pole and Moving Deformable Barrier Side Impacts" Tesinghua Science and Technology, ISN 1007-0214 PP 725-730 (2006).
- [7] Rachman Setiawan, Mohammad Rusyad Salim "Crashworthiness Design for an Electric City Car against Side Pole Impact" J.Eng. Technol.Sci., Vol.49, No.5, 2017, PP587-603.
- [8] Sandeep Dalavi, P.M.Ghanegaonkar, Tushar Salunkhe "Crashworthiness of Car Interior Door Trims in Side Impact- A Review" IJESIT, Vol4, Issue5 (2015). ISSN:2319-5967.
- [9] ANCAP Pole Side Impact Testing Protocol v7.0.2 (2018) .
- [10] NHTSA "Structural Countermeasure/Research Program: Mass and Cost Increase Due to Oblique Offset Moving Deformable Barrier Impact Test" US Department of Transportation (2018).